269600-14-T
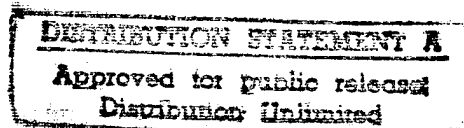
PRESENT STATUS OF SAR SEA ICE ALGORITHMS

June 1988

C. Wackerman
R. Jentz
R. Shuchman
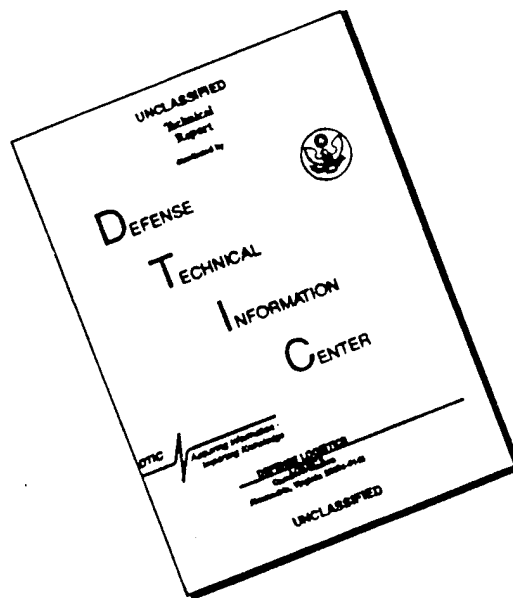
Radar Science Laboratory
Advanced Concepts Division
Environmental Research Institute of Michigan
Ann Arbor, MI 48107

19960719 053

DTIC QUALITY INSPECTED 4

DISCLAIMER NOTICE

THIS DOCUMENT IS BEST QUALITY AVAILABLE. THE COPY FURNISHED TO DTIC CONTAINED A SIGNIFICANT NUMBER OF PAGES WHICH DO NOT REPRODUCE LEGIBLY.

ERIM-320

REPORT DOCUMENTATION PAGE

1. AGENCY USE ONLY (Leave Blank)	2. REPORT DATE	3. REPORT TYPE AND DATES COVERED
	June 1988	Technical,

4. TITLE AND SUBTITLE

Present Status of SAR Sea Ice Algorithms

5. FUNDING NUMBERS

N00014-81-C-0295
N00014-88-C-0680

6. AUTHOR(S)

C. Wackerman, R. Jentz, R. Shuchman

7. PERFORMING ORGANIZATION NAME(S) AND ADDRESS(ES)

Environmental Research Institute of Michigan
P.O. Box 134001
Ann Arbor, MI 48113-4001

8. PERFORMING ORGANIZATION REPORT NUMBER

269600-14-T

9. SPONSORING/MONITORING AGENCY NAME(S) AND ADDRESS(ES)

Office of Naval Research
800 N. Quincy
Arlington, VA 22217

10. SPONSORING/MONITORING AGENCY REPORT NUMBER

11. SUPPLEMENTARY NOTES

12a. DISTRIBUTION/AVAILABILITY STATEMENT

unlimited

12b. DISTRIBUTION CODE

13.
This report will summarize the current work being done to extract geophysical information from Synthetic Aperture Radar (SAR) images of sea ice. There are many ways of organizing such a summary and we have chosen to divide it into three main areas; sea ice image classification, ice kinematics and sea ice image characterization. Image classification refers to algorithms that subset the pixels within an image based on an estimation of the type of sea ice (of course, we are including water as a type of sea ice) that pixel came from. Ice kinematics refers to algorithms that extract velocity vectors from the images that estimate the movement of the ice. Image characterization refers basically to everything else; i.e., algorithms that attempt to extract any other geophysical parameters from the images except ice type or ice motion.

For each of these areas we will describe the algorithms currently being applied, mention their advantages and disadvantages when known, and report any error analysis that has been performed to test how well the algorithms actually work. References will be given where we have found them, but much of this work is ongoing and thus has not been published but rather has been discussed at workshops or with individual communications.

14. SUBJECT TERMS

SAR, ice kinematics,

15. NUMBER OF PAGES 32

16. PRICE CODE

17. SECURITY CLASSIFICATION OF REPORT	18. SECURITY CLASSIFICATION OF THIS PAGE	19. SECURITY CLASSIFICATION OF ABSTRACT	20. LIMITATION OF ABSTRACT
unclassified	unclassified	unclassified	unlimited

1.0 INTRODUCTION

This report will summarize the current work being done to extract geophysical information from Synthetic Aperture Radar (SAR) images of sea ice. There are many ways of organizing such a summary and we have chosen to divide it into three main areas; sea ice image classification, ice kinematics and sea ice image characterization. Image classification refers to algorithms that subset the pixels within an image based on an estimation of the type of sea ice (of course, we are including water as a type of sea ice) that pixel came from. Ice kinematics refers to algorithms that extract velocity vectors from the images that estimate the movement of the ice. Image characterization refers basically to everything else; i.e. algorithms that attempt to extract any other geophysical parameters from the images except ice type or ice motion. Since ice type and motion are the dominant areas of research by far and very little work has been done in the other areas, we felt justified in discussing these other algorithms in one section.

There is, of course, much interplay between these areas; we do not mean to imply by this organization that the algorithms are necessarily independent. Ice kinematic algorithms often need to characterize a section of one image so as to track it to another image and this characterization is often perilously close to performing ice type mapping. Performing ice type classification on the whole image before performing ice kinematic estimations may help decrease search times in the kinematic algorithms. We are, rather, organizing the algorithms as to their main intent; i.e. the final output product that is driving the structure of the algorithm. Although this causes some overlap in the methods employed, we fell it gives a more natural segmentation.

For each of these areas we will describe the algorithms currently being applied, mention their advantages and disadvantages when known, and report any error analysis that has been performed to test how well the algorithms actually work. References will be given where we have found them, but much of this work is ongoing and thus has not been published but rather has been discussed at workshops or with individual communications. To insure that no major research area has been missed, and to expand the

details on the algorithms presented here, a series of discussions with the major researchers has been planned for the latter part of July. All additional information gathered during these discussions will be subsequently summarized.

Section 2 of this report will briefly present the background of the SAR sea ice algorithm research to provide a framework for the current research. Section 3 will discuss the ice type classification work, Section 4 will discuss the ice kinematics work and Section 5 will discuss the image characterization algorithms. Finally, Section 6 will discuss future directions that we believe will be taken in these areas. In addition, included as an appendix is a paper presented at IGARSS 87 which also summarized sea ice algorithms and was the initial source of information for this report. Although we have changed the organization slightly, the same information has been incorporated here along with the additional information that has been gathered.

2.0 BACKGROUND

Research into radar signatures of ice has been going on for over twenty years. The earliest works [1-4 for example; there is a lot of literature on this subject so all the references in this report are meant as samplings, not inclusive lists] established that radar returns did indeed differ for the various ice types and began to examine how changes in frequency, polarization and incidence angle affected the resultant image. A large amount of scatterometer data was collected [5-9] and used mainly to test ice type classification algorithms; i.e. to determine how well ice types could be differentiated using various radar parameters. Statistical analysis of single pixel backscatter intensities including cluster plots, probability density function estimation, hypothesis testing, etc. [10-13] were applied in order to determine algorithms that give the maximum separation for any given pair of ice types (see section 3 for a more detailed discussion of these algorithms). In general, the conclusions drawn from these studies were as follows. First, the character of the ice returns differed greatly from season to season. Summer conditions with the possibility of free water on the surface of the ice tend to make the

returns from varying ice types very similar and thus make differentiation very difficult. Winter conditions were much better since the ice types had more differing backscatter characteristics. Second, X-band data appeared to give the greatest difference in backscattered energy between ice and water. In fact, cross-polarized data gave the best results of all, but this required a lot of transmitted power to receive the signal. The X-band like-polarized data was very similar, however, but required less power, so it became the favorite data set for separating first year ice, multi-year ice and water. Third, L-band data exhibited the best textural differences between ice types, showing ridge lines and meltpools much better then the X-band, and gave more promise of being able to differentiate between ice types instead of simply differentiating between water and any other ice. Finally, C-band data was shown to fit midway between the X and L-band results; appearing very similar to L-band in summer conditions but more like the X-band during other times of the year.

Thus much research went into characterizing how SAR images of different polarization and frequencies respond to different ice types and in different seasons. Obviously, the next easiest step was to derive automatic algorithms to do the ice type classification and thus, as summarized in section 3, whole families of algorithms were tested on the data to perform that function [12-15]. Most of them were designed to make use of the image characterizations that researchers had previously observed visually and to simply automate the process. Eventually, however, it was recognized that it might be useful to derive algorithms that extract quantities other then SAR ice type directly from the SAR images and one such quantity of great interest was ice kinematics. Thus much research went into generating algorithms for measuring ice motion [16-18] (see section 4 for further discussion) and since the problems were investigated after the initial SAR image analysis described above, the research was based more on different aspects of the problem then on image characteristics that were visually observed by researchers. Section 4 is therefore organized more according to the research problems (detecting shifts, detecting rotations, etc.) then section 3.

Of course, ice kinematics is only one area of geophysical research, and a number of other algorithms for extracting lead locations [19], floe

sizes and floe shapes directly from the image have been developed and are discussed in section 5. Even these are just a few of the possibilities, and some possible future directions for SAR sea ice algorithms are discussed in section 6; more rigorous algorithm testing, use of the SAR phase information and characterization of pieces of SAR images for identification in other images are just some of the possible directions.

3.0 ICE TYPE CLASSIFICATION

As mentioned in section 2, this area received the earliest attention in SAR sea ice work since the first questions that researchers needed to answer were how the backscattered returns differed for the various ice types. In addition, a lot of useful geophysical information can be extracted from an accurate ice type map and this further spurred activity; ice concentration, ice floe differentiation, lead location, lead shape characterization and ice floe distributions are just some examples. As noted above, this research was driven more by the visual characterization of the SAR images and the algorithms that were developed tried to exploit those attributes. One possibility, therefore, for organizing these algorithms is under the three catagories: (1) algorithms based on individual pixel intensities; (2) algorithms based on local pixel intensities (or texture analysis); (3) other techniques which will include supervised methods and expert systems. The first category represent algorithms which try to characterize the ice types based on the behavior of the intensity of individual pixels. The second category represents algorithms which make use of spatial relationships in the pixel intensities; these characteristics often being referred to as texture. The final category is basically all the other algorithms.

Algorithms in the first category can be further broken down into three types; simple thresholding, adaptive thresholding and statistical comparisons. Simple thresholding is based on the assumption that the ice types can be characterized by a difference in their mean intensity values. Thus an ice type map can be produced simply by deciding the intensity ranges that each ice type occupies and thresholding the image accordingly. In actual implementation, such algorithms usually require some noise

smoothing first in order to reduce the variation in intensities from any given ice type (especially considering the speckle characteristics of SAR imagery). Also, they assume that the data has already been radiometrically corrected, since gain changes due to antenna patterns or range fall-off effects make such global thresholding operations useless. The threshold values are usually determined from histograms of the total image. If such histograms display obviously separated areas the threshold determination is easy; more often the histogram needs to be massaged or a threshold guessed at since the histogram is usually unimodal. Figure 1, illustrates the unimodal nature found in unaltered SAR sea ice images. It would be extremely difficult to determine a threshold location from this image. Figure 2, shows the same image after the above described corrections have been made, here the threshold location is obvious.

That differences in backscattered intensities can be used to determine ice type has been demonstrated on scatterometer data [11] and has been used successfully on SAR data to estimate ice concentration [13,20]. The ice concentration work, when compared to manually interpreted data, showed a 14% error [20]. The so called "mixed pixel" problem, where a single SAR resolution cell return can be composed of partial ice and partial water returns, can also be addressed by using the histogram to estimate the percentage of ice/water pixels [20]. In general, simple thresholding has been shown effective in distinguishing ice and water (i.e., performing ice concentration) on images that have had their noise reduced, and are radiometrically correct. This is illustrated in figure 2. Simple thresholding appears to be inadequate for distinguishing between different ice types due to the large overlap region in intensity values that most ice types share.

To address some of the drawbacks of simple thresholding, algorithms based on adaptive thresholding have been investigated. These algorithms use a small, local histogram to establish a threshold only for that local area, then move to the adjacent local area to determine a possibly different threshold. These algorithms are driven by the observation that local histograms taken over the border between two different ice types will appear bi-modal even when the total image histogram is still unimodal and thus can be used locally to segment the image. This is demonstrated in

figure 3 which contains two local histograms one over an ice area and the
other over an ice/water border. Notice that the local histogram of the
ice/water border area is bimodal and can be used to seperate this local
area into its two corresponding types. Also, notice that the global
histogram of this image ,shown in figure 1, is unimodal. Additionally,
these algorithms have an advantage in that the statistics of the classes
can be allowed to drift slightly (i.e. the threshold that separates two ice
types can be different for the near range sections of the image then for
the far range sections) thus alleviating the need for strict radiometric
correction. These algorithms are just being investigated, so no error
analysis is available yet. Figure 4, shows an example of this local
histogram segmentation (adaptive) algorithm on synthetic data along with a
threshold map produced by the global thresholding algorithm.

It should be noted that although the adaptive thresholding algorithms
discussed above and the statistical approaches discussed below actually
rely on information from pixels within a local area, they are included in
this section on individual pixel algorithms instead of the later section on
local pixel algorithms because the algorithms are based on the assumption
that the pixel intensities are identically distributed and independent,
thus the local operations are simply to derive estimates of the single
pixel parameters that have less noise. This is to be contrasted to the
algorithms that will come later which depend on their being some spatial
correlations between pixels; i.e. that they are not identically distributed
and independent.

A third type of algorithm in this class is based on the statistics of
the pixel intensities. Cluster plots of the mean backscatter values for
different polarizations or frequencies for scatterometer data have been
seen to divide the returns into classes that correspond to different ice
types [11], this is illustrated in figures 5 and 6. Recently a cluster
plot of local mean versus local variance from a SAR image has been shown to
distinguish between open water and ice sufficiently to allow lead location
determination with a 20% error as compared to manual interpretation [17].
Figure 7, shows a cluster plot of local mean versus local variance from the
image shown in figure 8 (Rev. 1482). It has been shown that the higher
order statistics (third order or higher) probably contain very little

discriminating ability [12] and thus the mean and variance may be as far as one should go. Further, it has been proposed that the histograms derived from different ice types do not display any statistical differences [12] and thus could not be used as classifier.

A second class of algorithms are ones based on local pixel intensities (i.e. the local, spatial relationship between pixel intensities), often called texture analysis. As mentioned above, these algorithms attempt to exploit any spatial correlations in the images, and initially were prompted by the observations that L-band data contained a lot of texture information in the form of ridge lines and meltpools that seemed to visually distinguish between ice types.

The most promising texture measure to data has been the co-occurrence matrix [21]. Briefly, the user specifies a vector which represents a separation between two pixels and then forms a 2-D matrix whose rows and columns represent all possible intensity values for any pixel and whose entries are the percent occurrence in the image of two pixels, separated by the specified vector, and having the corresponding row and column values. Obviously, there is a co-occurrence matrix for each possible vector separation. What these matrices are measuring is the spatial correlations within the image; thus they are very good in locating ridge lines, or any other directional aspect. It is, however, extremely computationally intensive to generate these matrices, but what you gain is a great deal of flexibility; in fact a large number of operations have been designed for these matrices [21] to extract a single value to use in classification that corresponds to how peaked the matrix is along the diagonal, how evenly spread out the values are, where the highest concentration of pixel pairs lie, etc. Thus a lot of texture information can be measured by applying operations to these co-occurrence matrices, and using the so-called inertia measure [21] on cross-polarized X-band data, ice classification between first, second and multiyear ice was done with a 35% error based on manual interpretation [14].

Another algorithm to exploit spatial correlations makes use of the Fourier transform. By integrating the energy in various subsets of the Fourier domain such as annuli, wedges or straight lines that go through the origin, the energy in features that have a given spatial relationship (such

as a specified frequency but any orientation, or a specified orientation and any frequency) can be calculated [15]. The rate of fall-off of the Fourier transform magnitude with frequency (where integration over angle was used to remove angular dependence) has been shown to be well correlated with ice concentration, however these results are still being investigated and have not yet been published (this work is being researched mainly at ERIM). In general, this algorithms show promise and they are much more computationally efficient then the co-occurrency matrices, although they lack the latter's flexibility.

A third texture algorithm models the image as an autoregressive process and uses the coefficients of that process to classify the data. As in the previous methods this algorithm is exploiting any spatial correlations, but further it is assuming those correlations can be modeled with an all pole filter. Initial results (this is being pursued mainly at JPL) show good classification when compared visually with the SAR image, but no published results are available yet.

A final set of algorithms make use of the two dimensional autocorrelation of the total image. Obviously, the shape of this autocorrelation will contain information on the shape of correlated pixels within the image. Such an approach has been used to locate and characterize leads (i.e. give their shape, orientation and the average distance between them) in ice imagery and gave good results when visually compared [19]. The 2-D shape of the autocorrelation function has been fit to an ellipse and the parameters of the ellipse have been used to characterize ice floe shapes (this has been done mainly at ERIM). Both these algorithms however, belong really to the image characterization discussion (Section 5) since they are not measuring ice type and so will be mentioned there again.

Finally, some other algorithms which really do not fall into any category have also been researched. Supervised classification algorithms which make use of a priori data about specific ice classes (usually the means and variances or the density functions) have been used (mainly at JPL) though no results are available yet. Also, an expert system approach using a rule-based algorithm is being investigated (at the University of Kansas) where the rules are being derived from interviews with SAR image

analysts; no results for this approach are available yet either.

The current state of ice classification algorithms can be summarized as follows. Ice concentration (i.e. separating ice images into simply ice and water) seems to be well in hand using X-band (preferably cross-polarized) winter data and perform simple thresholding or segmentation based in means and variances. Distinguishing between different ice types still needs more effort, but a promising texture approach appears to be co-occurrency matrices, while adaptive thresholding appears to hold promise as a "statistical" approach. Obviously, more error analysis needs to be done on all the algorithms and they need to be tested on data from a variety of seasons since it may become necessary to use different algorithms for images from different seasons. Also, it appears that statistics higher then the second order will not be very useful and that some amount of noise smoothing will have to be done before performing any classification, although some of the adaptive algorithms may allow a relaxing on the need for radiometric correction.

4.0 ICE KINEMATICS

As mentioned above, work on ice kinematics came after the initial burst of activity on ice segmentation, so the areas of research are more defined along the research problem boundaries as opposed to being driven by image characteristics. We have divided the discussion therefore into three areas; use of manual or computer aided interpretation, automatic detection of shifts, and automatic detection of rotations.

The problem in ice kinematics is, of course, to automatically derive velocity vectors for the ice motion. It was recognized early on that the problem contains different aspects depending on where the image was taken. Ice motion within the ice pack was almost always strictly translational; very little rotation occurred although there was some deformation of the ice in its movement. The marginal ice zone was very different however since the ice floes rotated, broke apart and merged together rather regularly in addition to translating. This was obviously noted as being the more difficult area to perform ice kinematics automatically, so almost all the work to data has been on data from the ice pack and on detection of

translational motion (strictly shifting of the image). Some work however has just recently been done on the problem of rotation detection, although to date it has been applied strictly to images within the ice pack.

Manual interpretation of the data to determine ice movement vectors was the first approach and is, of course, the most straightforward. The human interpreter is much more able to detect the same ice patch or ice floe in two separate images even if it has rotated and deformed in addition to shifting. Most manual interpretation (performed mainly at ERIM) uses SAR images that have been collected over very large areas in a stripmap mode and this usually implies optically processed data since the digital processing algorithms do not lend themselves to generating such large quantities of data. Figure 9 illustrates a vector field and ice edge generated from optically processed stripmap SAR data gathered during the 1984 Marginal Ice Zone Experiment (MIZEX-84). It shows both the motion and shape of the ice edge as it changed from June 29 to July 6. More recently, computer programs have been developed (mainly at JPL) that allow users to display images, locate the same points in each image, then allow the computer to determine the velocity vectors from those points. This combines the advantages of the human interpreter image processing capability with the computer power for performing the straightforward manipulations. Unfortunately, this requires digital data and thus does not have the advantage of manually scanning large tracts of optical data.

Although a large number of researchers have been working on the problem of automatically detecting shifts (mainly, as mentioned above, using data within the ice pack), unlike the ice segmentation work an almost unified algorithm appears to have emerged. Unfortunately, most of this work is very current and not much has been published; [16,18] give some overview and in what follows we shall include the researcher and the institute on the results that we state. The first problem is to locate the same ice patch within two images that are separated in time. It is generally agreed that some pyramid approach is necessary to make the algorithms computationally possible. Although some differ in details, all such approaches generally correlate the two images on a very gross scale first to locate areas having higher correlation, then look within those areas to determine finer estimate of the shifts. Although the cross-

correlation function is usually used, some indication have been given that a finite gradient measure is less noisy and that some noise smoothing operations applied beforehand can help the algorithms (Emery and Collins, UBC). Although these techniques only handle shifts it has been calculated that rotations $<$ 15 degrees will still allow them to work (Vesecky, Stanford) without significant degradation. A number of images, mainly SEASAT data, has been used to test the algorithms (although ground truth to compare against is somewhat lacking in this area) and the results look very good. Figure 8, shows two SEASAT images used for this analysis. Figure 10, shows three different resolutions of the image REV. 1482 which are used to determine estimates of the shifts. Figure 11, illustrates the displacement vector fields for the different resolution images shown in figure 10.

With the shift detection well in hand, the next problem is automatic detection of rotations. As mentioned above, rotations $>$ 15 degrees can cause considerable difficulties when detecting similar ice patches using cross-correlations, so some means of allowing for rotations needs to be considered. One approach is to explicitly rotate the image by a set of incremental values and perform the cross-correlation on each, using the peak cross-correlation output as the indicator of the rotation value (Strong, GSFC). This is, however, computationally intensive and so algorithms to detect the same ice patch in another image that are insensitive to rotations of that ice patch are being investigated. One such approach is to characterize the ice patch by moments that are invariant to rotation (Vesecky, Stanford; Lee, JPL), although these can also be somewhat hard to compute and may not differentiate between ice patches within the same image sufficiently. A second approach is to use an edge definition to characterize the ice patch which is also rotationally invariant (Vesecky, Stanford) although this implies a method of locating the edges with sufficient accuracy. In general, automatic detection of shifts is a relatively new area of research and not much can yet be said on the accuracy of any of the algorithms.

In summary, the ice kinematics algorithms are much less scattered then the ice segmentation algorithms; a few very definite approaches are being studied. The estimation of motion vectors for ice images within the ice pack is well established since the ice motion is mainly translational and

good, automatic algorithms exist. These usually involve a pyramid of cross-correlations to locate similar ice patches and limit search areas. Handling rotation or images from the marginal ice zone is still in its earliest stages; no good algorithms yet exist.

5.0 ICE IMAGE CHARACTERIZATION

All of the algorithms collected here have been discussed previously, but we thought it useful to collect them again under this heading. In the previous two sections we have emphasized two ice problems; ice type classification and ice motion determination. In this section, we will briefly mention the algorithms that extract other information from the SAR images. This is a relatively new area of research, segmentation and kinematics have dominated the research field for a while, and is often difficult to separate from the others; they will in fact share many of the same algorithms. But the information they are trying to extract is different and represent a new direction in SAR ice algorithm development; trying to estimate some specific geophysical parameter directly from the SAR image.

Two main algorithms have been developed. The first, mentioned in Section 3, is to locate and characterize lead locations [19]. This algorithm first creates a binary image to indicate ice and water (and thus really starts as an ice segmentation algorithm) then uses the shape of the main lobe of the autocorrelation to estimate the average shape of the lead and the location of the secondary peak to estimate the mean distance between leads. Ground truth to compare against in this area is somewhat lacking, but good visually compared results were obtained. Results from this algorithm are shown in figure 12. Figure 12a is a STAR-1 image used for this analysis, figure 12b shows the binary image, figure 12c is a contour plot of the autocorrelation of the binary image, and figure 12d is a reproduction of the lead locations. The second main algorithms try to extract mean floe shape and mean floe density. The mean floe shape can be extracted very similarly to the lead characterization. The half-power shape of the main lobe of the autocorrelation function is extracted and fit to an ellipse; the shape of the ellipse then estimates the average shape of

occurrency matrix perhaps) may be needed to further distinguish between ice types.

Future algorithms in ice kinematics will obviously need to be directed towards generating methods of characterizing ice patches that allow for both translational and rotational detection. These algorithms will have to be applied to the marginal ice zone also, so perhaps some method of handling deformation (floes that break up or merge) will need to be added although this may merely be finding a characterization that looks for features that remain constant (ridge line structures or meltpool locations perhaps).

In general, a good start has been made in creating automatic methods of extracting sea ice parameters. Ice concentration and ice translation detection appear to be well in hand and the current research efforts are directed towards fine tuning these algorithms, modifying them for wider application, and generating new algorithms in the harder areas.

REFERENCES

1. Anderson, V.H., "High altitude side-looking radar images of sea
    ice in the arctic," in Proc. Fourth Symp. on Remote Sensing of
    Environment, Univ. of Michigan, pp. 845-857, 1966.

2. Johnson, J.D., L.D. Farmer, "Use of side-looking radar for sea ice
    identification," J. Geophy. Res., vol. 76, no. 9, pp. 2138-2155,
    1971.

3. Dunbar, M., W.F. Weeks, "The interpretation of young ice forms in
    the Gulf of St. Lawrence using radar and IR imagery," DREO Rep.
    No. 711, Research and Development Branch, Department of National
    Defense, Ottawa, 40 pp., 1975.

4. Ketchum, R.D., "An evaluation of side-looking radar imagery of sea
    ice features and conditions in the Lincoln Sea, Nares Strait and
    Baffin Bay," NORDA Tech. Note 7, 1977.

5. Rouse, J.W. Jr., "Arctic ice type identification by radar," Proc.
    IEEE, vol. 57, pp. 605-611, 1969.

6. Parashar, S., R.M. Haralick, R.K. Moore, A.W. Biggs, "Radar
    scatterometer discrimination of sea ice types," IEEE Trans.
    Geosci. Electron., vol. GE-15, pp. 83-87, 1977.

7. Onstott, R.G., R.K. Moore, W.F. Weeks, "Surface-based
    scatterometer results of arctic sea ice," IEEE Trans. Geosci.
    Electron., vol. GE-17, pp. 78-85, 1979.

8. Onstott, R.G., C.V. Delker, "Radar backscatter study of sea ice in
    the Beaufort Sea," Remote Sensing Lab., Center for Res., Univ. of
    Kansas, Rep. 331-10, 30 pp., 1979.

9. Onstott, R.G., R.K. Moore, S. Gogineni, C. Delker, "Four years of
    low-altitude sea ice broad-band backscatter measurements," IEEE J.
    Oceanic Eng., Vol. OE-7, No. 1, pp. 44-50, Jan. 1982.

10. Larson, R.W., J.D. Lyden, R.A. Shuchman, R.T. Lowry,
    "Determination of backscatter characteristics of sea ice using
    synthetic aperture radar data," ERIM Final Report 142600-1-f, 110
    pp., 1981.

REFERENCES (cont.)

11. Gray, A.L., R.K. Hawkins, E.E. Livingston, L.D. Arsenault, M.W. Johnstone, "Simultaneous scatterometer and radiometer measurements of sea-ice microwave signature," IEEE J. Oceanic Eng., vol. OE-7, pp. 20-32, 1982.

12. Lyden, J.D., B.A. Burns, A.L. Maffett, "Characterization of sea ice types using synthetic aperture radar," IEEE Trans. Geosc. Remote Sensing, vol. GE-22, No. 5, Sept. 1984.

13. Burns, B.A., R.A. Shuchman, P.L. Jackson, J.D. Lyden, "SAR measurements of sea ice properties during MIZEX '83," IGARSS '84 SYMPOSIUM, Strasbourg, Aug. 1984.

14. Holmes, Q.A., D.R. Nuesch, R.A. Shuchman, "Textural analysis and real-time classification of sea-ice types using digital SAR data," IEEE Trans. Geosc. Remote Sens., vol. GE-22, No. 2, Mar, 1984.

15. Burns, B.A., D.R. Lyzenga, "Textural Analysis as a SAR classification tool," Electromagnetics, vol. 4, pp. 309-322, 1984.

16. Ninnis, R.M., W.J. Emery, M.J. Collins, "Automated extraction of pack ice motion from advanced very high resolution radiometer imagery," Journal of Geophysical Research, vol. 91, No. C9, pp. 10,725, 10,734, Sept. 15, 1986.

17. Fily, M., D.A. Rothrock, "Extracting sea ice data from satellite SAR imagery," to be published.

18. Fily, M., D.A. Rothrock, "Sea ice tracking by nested correlations," to be published.

19. Lyden, J.D., R.A. Shuchman, "A digital technique to estimate polynya characteristics from synthetic aperture radar sea-ice data," Journal of Glaciology, vol. 33, No. 144, pp. 243-245, 1987.

20. Burns, B.A., D.J. Cavalieri, M.R. Keller, W.J. Campbell, T.C. Grenfell, G.A. Maykut, P. Gloersen, "Multisensor comparison of ice concentration estimates in the marginal ice zone," Journal of Geophysical Research vol. 92, No. C7, pp. 6843-6856, June 30, 1987.

21. Haralick, R., "Statistical approaches to texture," Proc. IEEE, vol. 67, pp. 786-804, May 1979.

ERIM

APPENDIX A

PROGRESS ON DIGITAL ALGORITHMS FOR DERIVING

SEA ICE PARAMETERS FROM SAR DATA

PROGRESS ON DIGITAL ALGORITHMS FOR DERIVING
SEA ICE PARAMETERS FROM SAR DATA

R.A. Shuchman, B.A. Burns, C.C. Wackerman,
R.G. Onstott, and J.D. Lyden

Radar Science Laboratory
Advanced Concepts Division
Environmental Research Institute of Michigan
Ann Arbor, MI   48107

Over the past several years research on SAR sea ice imagery has focused on determing whether information on ice field parameters, including ice type, ice concentration, density and sizes of leads, and floe size distribution, could be obtained from the SAR data. This research has shown promising results and produced an extensive SAR signature data base as well as rudimentary algorithms for obtaining these parameters. With the advent of operational SAR satellite systems, it becomes even more important to develop this capability to monitor ice conditions in the Arctic in support of navigation, exploitation, and climatology. Therefore the focus of the SAR research has now shifted to the development of efficient automatic and almost real-time algorithms. In this paper we present an overview of the progress made in the development of these algorithms.

The approaches taken to construct algorithms for deriving the various sea ice parameters are summarized in Table 1. The two key elements in these approaches are image segmentation and statistical analysis in either the image or Fourier domain. For example, an algorithm developed to derive lead statistics segments the image based on the difference in intensity between ice and open water, and then uses characteristics of the autocorrelation of the segmented image to obtain lead dimensions, spacing and density [1]. As indicated in Table 1, algorithms for ice type, ice concentration, and lead statistics are using primarily fully digital approaches, whereas ice kinematics and floe size distribution algorithms at present still rely heavily on a combination of manual interpretation, to arrive at the segmented image, and computer analysis of the manually derived image data. Fully digital approaches for these two sea ice parameters are being pursued in parallel. Algorithms have yet to be developed for determination of ridge statistics or ice thickness from SAR data. Of the possible approaches listed in Table 1, many would make use of the phase as well as the intensity information contained in the SAR signal, allowing, for example, ice floe motion to be derived on the basis of the Doppler shift imparted to the returned signal.

The progress made to date on development of digital SAR sea ice algorithms is summarized in Table 2. Here we consider four stages in algorithm development: 1) understanding of the physical basis for deriving the sea ice parameter; 2) translation of that understanding into a mathematical model; 3) implementation of the mathematical model into a computer algorithm; and 4) validation of the algorithm.

The physical basis for deriving most of the sea ice parameters from SAR data is the large contrast between radar cross sections of ice and open water [2,3]. This characteristic alone is a sufficient basis for lead and floe size distribution and total ice concentration algorithms in most imaging situations [1,4,5]. For ice type discrimination and fractional concentration algorithms, additional information is required. Local image texture and the statistics of SAR intensity, which have been shown to be useful in discriminating floes of different ice types and degrees of deformation [6,7], have been exploited for these algorithms. Both ice/water contrast and texture within floes are used as the basis for ice kinematics algorithms involving manual interpretation [4], but to date the digital algorithms make use of the textural characteristics of the entire scene such as linear features and persistent patterns [8,9]. In the case of deriving ridge statistics, we do not as yet completely understand the physical mechanism for SAR imaging of ridges making it difficult to generalize ridge signatures in a way that could be quantified. Ice thickness is the extreme case where it is not known if SAR can provide this information.

A major step in algorithm development is the transition from the physical basis to a mathematical model and its implementation in a digital algorithm. At this step it is to some extent necessary to quantify the methodology of a human interpreter in such a way that the method can be implemented within a computer architecture. For ice/water and ice type discrimination, the mathematical model consists of a hierarchy of intensity and texture measures associated with the various scene components. These descriptive measures are generated from the SAR and scatterometer signature data bases and account for both natural variations in ice surface conditions and speckle-related variations. An algorithm is then implemented that compares local image statistics to these measures. At this stage segmented images can be obtained (i.e. ice type or ice concentration maps) [10,11]. Subsequent processing is needed for floe size and lead statistics. Fourier transform techniques, specifically the characteristics of the autocorrelation function, have been found useful for obtaining lead orientation and density information, but less useful for floe size. For floe size determination, a mathematical model must still be determined that will quantify boundary information efficiently. Pattern recognition type techniques are being investigated for this purpose and for ice kinematics algorithms since shape and context information are so important in manual interpretation of SAR imagery. These manipulations may be facilitated by the use of parallel-processor computer frameworks such as that of the ERIM cyto-computer [12].

Algorithm validation, i.e. comparison with independent measures of the sea ice parameter of interest, has been carried out for the ice type, ice concentration, and lead distribution algorithms only. The ice type and lead distribution algorithms have been exercised on single SAR scenes for which ice surface observations were available. The ice concentration has been the most extensively validated by comparing concentration estimates to those derived from near-simultaneous passive microwave data and aerial photography [13], but under summer MIZ conditions only. Lack of SAR imagery with sufficient spatial and seasonal coverage is at present a limiting factor in validation efforts.

Table 1. SAR Sea Ice Algorithm Approaches

Sea Ice Parameter	Current Algorithm Approaches	Possible Algorithm Approaches
Ice Type	Image Segmentation -pixel intensity -neighborhood texture	Multivariate Complex Data
Ice Concentration	Image Segmentation Statistical Analysis Fourier Analysis	Combination with Passive Data
Lead Distribution	Image Segmentation + Autocorrelation	Complex Data
Ice Kinematics	Manual Interpretation + Computer-generated vector fields Pattern Recognition + Autocorrelation	Single and Multiple Frame Doppler Analysis
Floe Size Distribution	Manual Analysis + Computer-generated satistics	Pattern Recognition
Ridge Statistics		Edge Detection
Ice Thickness		?

Table 2. Progress on Digital SAR Sea Ice Algorithms

Sea Ice Parameter	Physical Basis Understood	Mathematical Model	Algorithm Implemented	Algorithm Validated
Ice Type	yes	yes	yes	limited
Ice Concentration	yes	yes	yes	summer only
Lead Distribution	yes	yes	yes	limited
Ice Kinematics	yes	under development	under development	no
Floe Size Distribution	yes	no	no	no
Ridge Statistics	no	no	no	no
Ice Thickness	no	no	no	no

REFERENCES

1. Lyden J D & Shuchman R A 1987, A Digital Technique to Estimate Polynya Characteristics from Synthetic Aperture Radar Sea Ice Data, J. Glaciology (in press).

2. Gray A et al. 1982, Simultaneous scatterometer and radiometer measurements of sea-ice microwave signatures, IEEE J. Oceanic Eng., OE-7, 20-32.

3. Onstott R G & Gogineni S P 1985, Active Microwave Measurements of Arctic Sea Ice Under Summer Conditions, J. Geophys. Res., 90, 5035-5044.

4. Burns B A et al. 1985, Computer-Assisted Techniques for Geophysical Analysis of SAR Sea-Ice Imagery, Proc. 19th Int. Symp. Rem. Sensing, Ann Arbor, MI, 947-959.

5. Fily M & Rothrock D 1985, Extracting Sea Ice Data from Satellite SAR Imagery, IGARSS'85, Amherst, MA.

6. Lyden J D, Burns B A & Maffett A L 1984, Characterization of Sea Ice Types Using Synthetic Aperture Radar, IEEE Trans. Geosc. Rem. Sensing, GE-22, 431-439.

7. Burns B A & Lyzenga D R 1984, Textural Analysis as a SAR Classification Tool, Electromagnetics, 4, 309-322.

8. Curlander J C, Holt B & Hussey K J 1985, Determination of Sea Ice Motion Using Digital SAR Imagery, IEEE J. Oceanic Eng., OE-10, 358-367.

9. Vesecky J F et al. 1986, Automated Remote Sensing of Sea Ice Using Synthetic Aperture Radar, Proc. IGARSS'86, Zurich, 127-132.

10. Holmes Q A, Nuesch D R & Shuchman R A 1984, Textural Analysis and Real-Time Classification of Sea-Ice Types Using Digital SAR Data, IEEE Trans. Geosc. Rem. Sensing, GE-22, 113-120.

11. Burns B A et al. 1984, SAR Measurements of Sea Ice Properties During MIZEX'83, Proc. IGARSS'84, Strasbourg, 347-351.

12. Lougheed R M & McCubbrey D L 1980, The Cytocomputer: A Practical Pipelined Image Processor, Proc. 7th Int. Sym. Computer Architecture.

13. Burns B A et al. 1987, Multisensor Comparison of Ice Concentration Estimates in the MIZ, J. Geophys. Res., (in press).
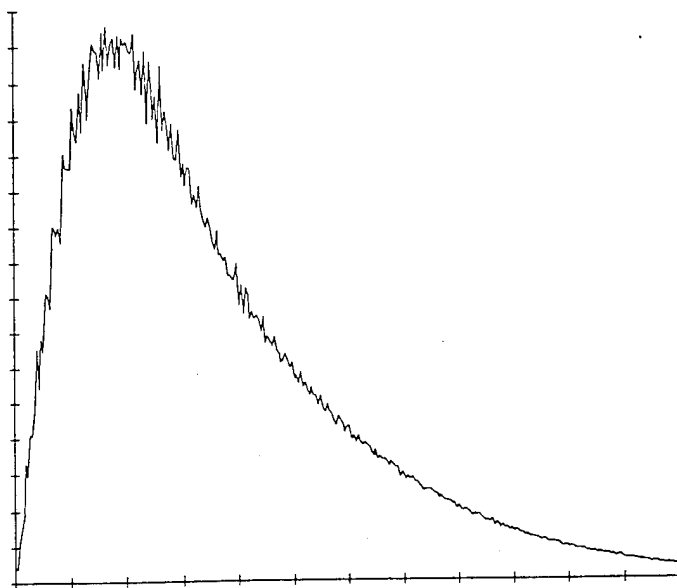
Figure 1. Global histogram of a SAR sea ice image.
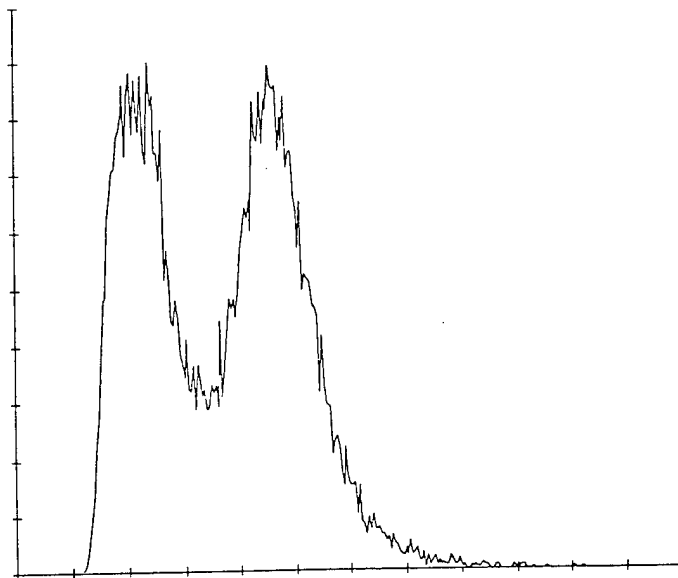

Figure 2. Global histogram of a SAR sea ice image after a
smoothing algorithm was applied to reduce system noise.
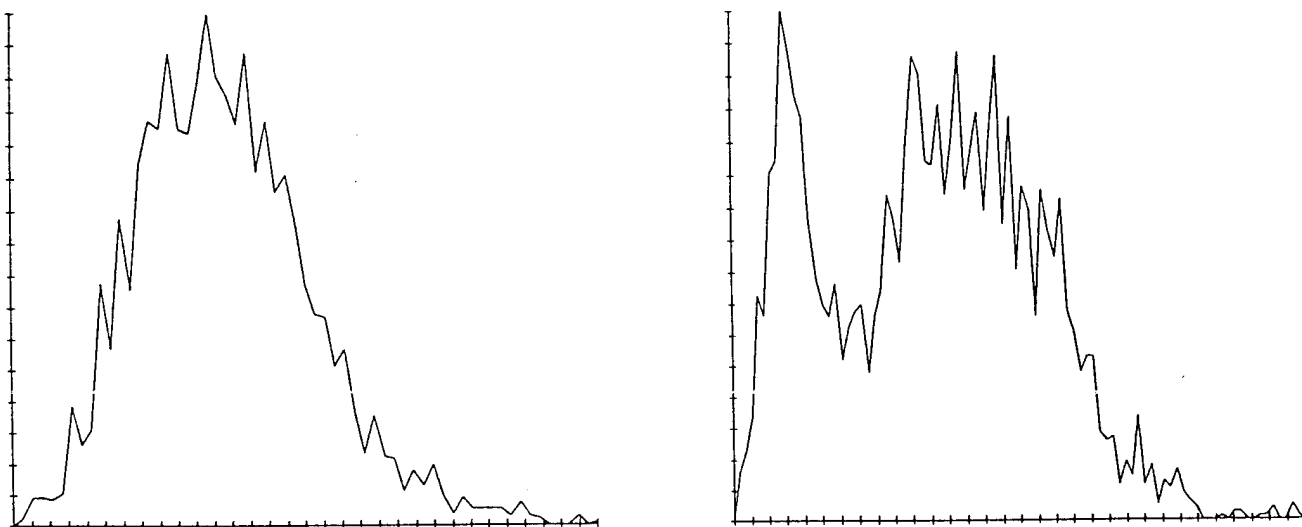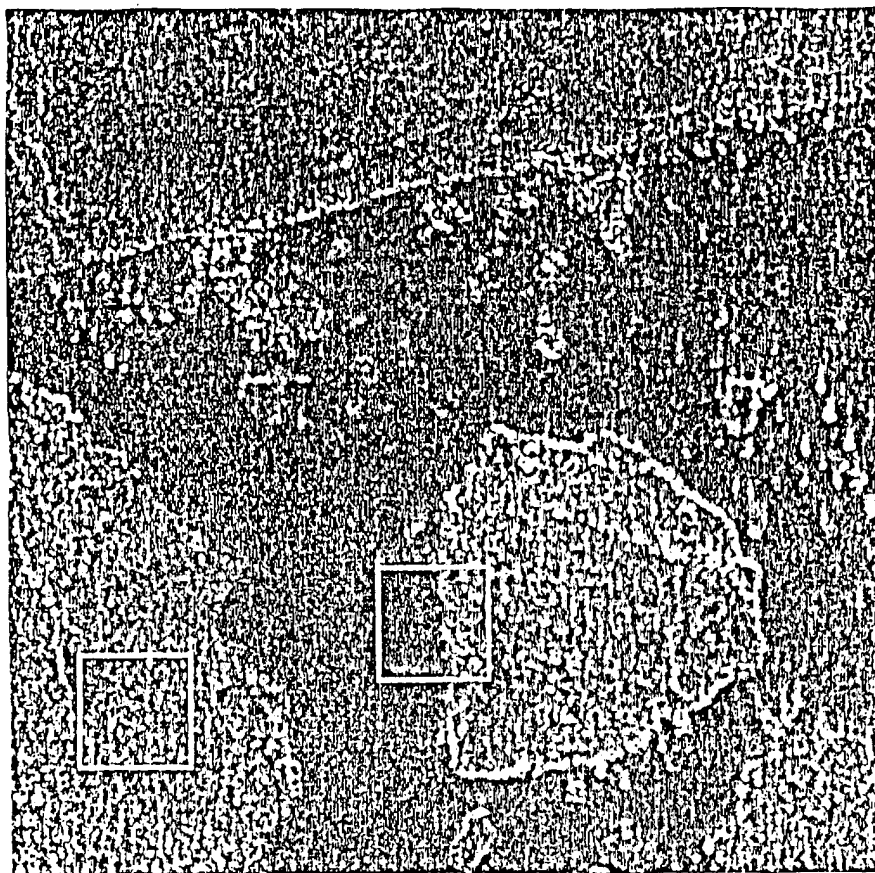
GENERATE LOCAL HISTOGRAM

Figure 3. Local histograms of a SAR image. Edges may be detected
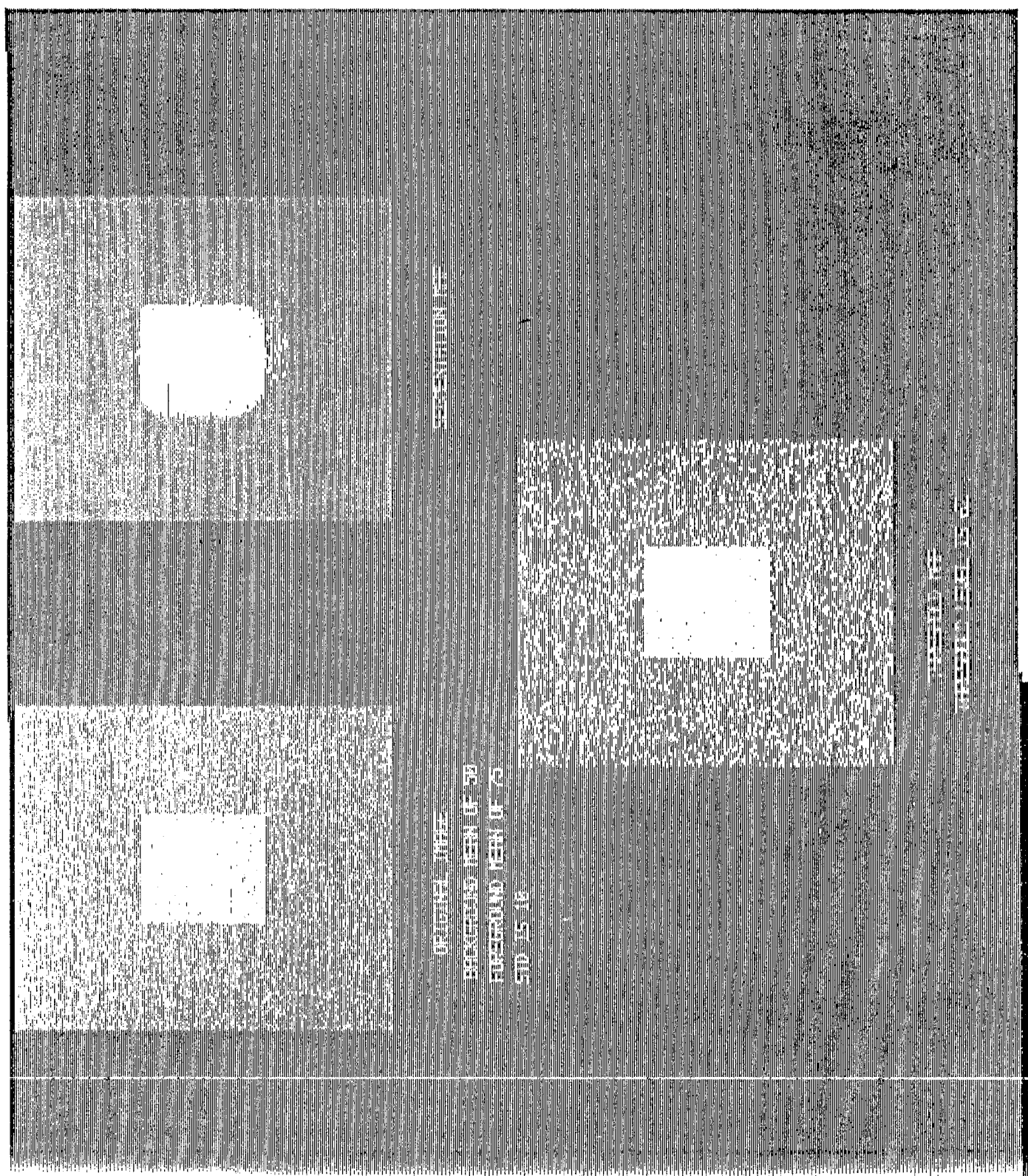when the histogram is bimodal.

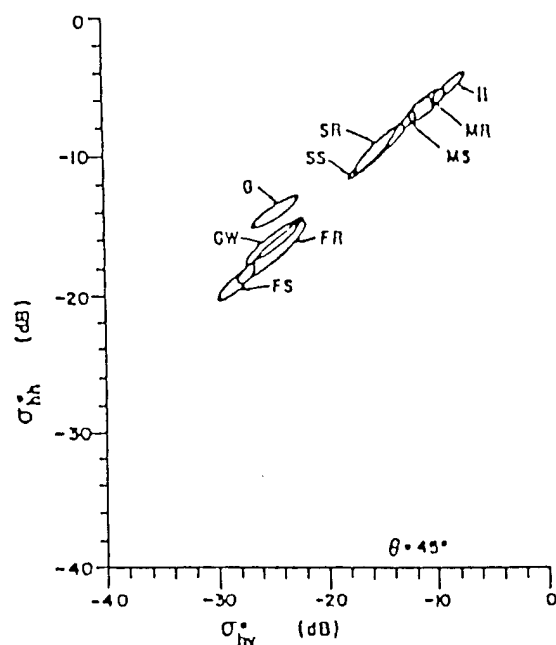Figure 4. Example of local histogram segmentation algorithm on synthetic data.

Fig. 5. Ku-band backscatter coefficient distribution envelopes from Beaufort Sea ice in the March, 1979 period. The hyperspace ellipses are standard deviation contours for each of the classes shown. The ice class symbols are: G—grey, G-W—Grey white, FS—smooth first-year, FR—rough first-year, SS—smooth second-year, SR—rough second-year, MS—smooth multi-year, MR—rough multi-year, II—Ice Island. Substantial overlap can be seen in the ellipses for the rough and smooth subclass of second-year and multi-year ice, and for grey-white and rough first-year ice. A very clear separation is present between old ice and first-year and younger ice classes in either polarization, but additional contrast is available in a cross-polarized mode.
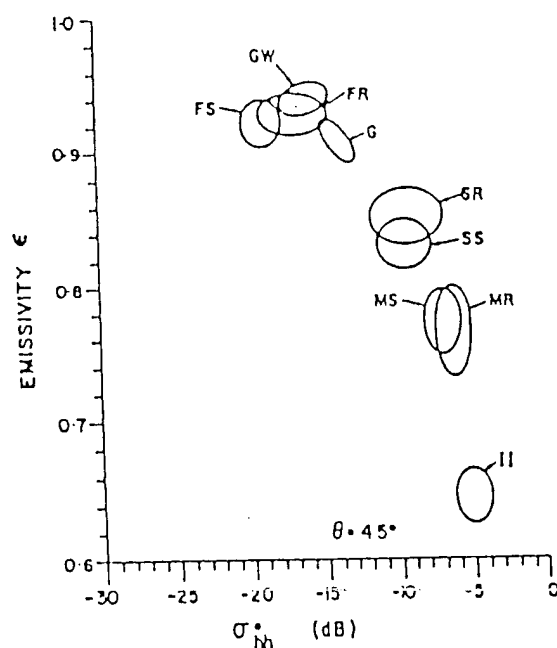
Fig. 6. Ku-band backscatter coefficient and K-band emissivity distribution envelopes from Beaufort Sea ice in March, 1979. These hyperspace distribution contours demonstrate the advantage of a combined active/passive measurement to separate sea ice classes. Clearly the emissivity data give added separation to the ellipses for the old ice classes as can be observed from a comparison of Figs. 5 and 6.
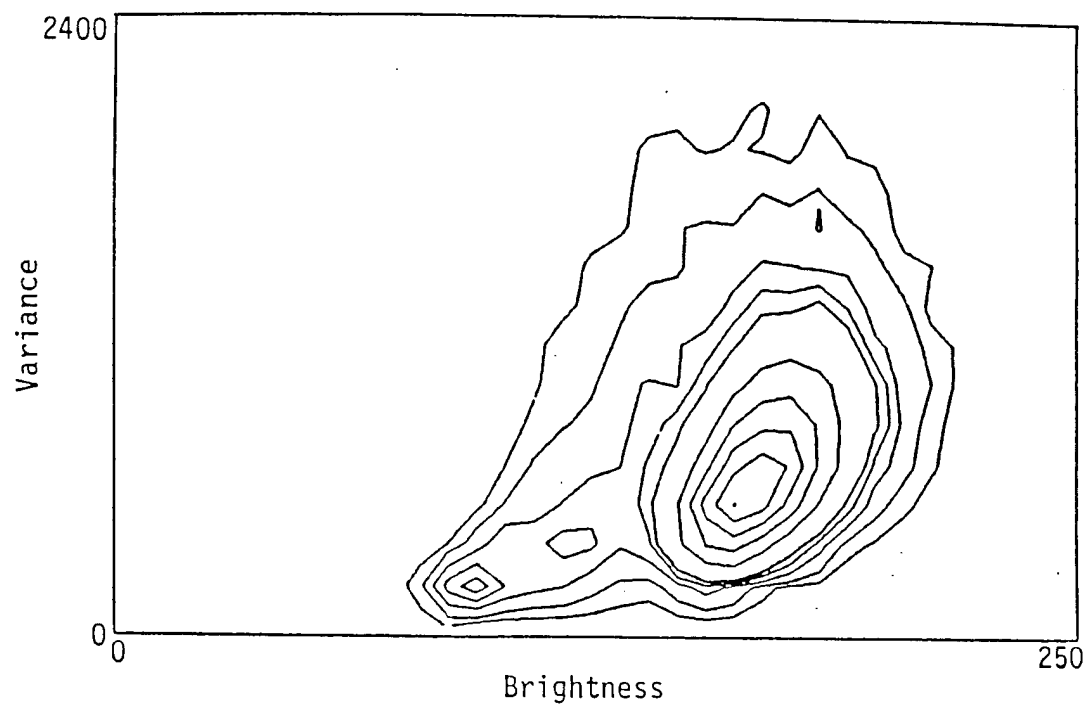
Figure 7. Distribution of brightness and variance for the big
pixels derived from the data in figure 8.

Fily and Rothrock
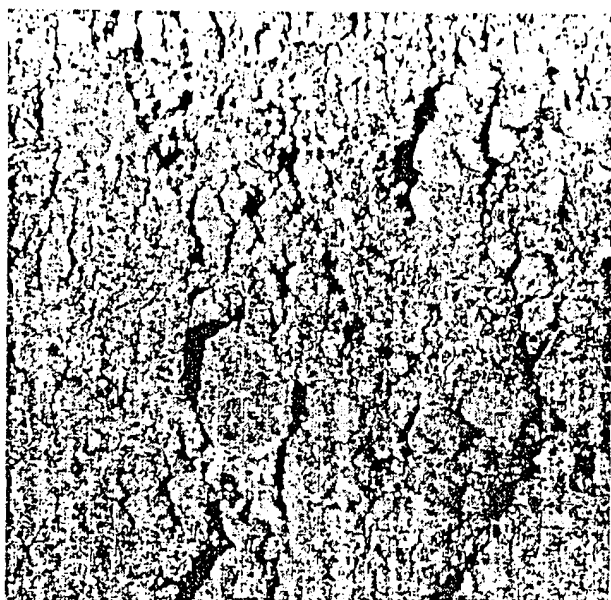
Rev. 1439

Rev. 1482

Figure 8. SAR images from SEASAT Revs. 1439 and 1482. In this and
all derived figures, sample number (distance along
track) increases to the right, and line number (and
range) increases from top to bottom.

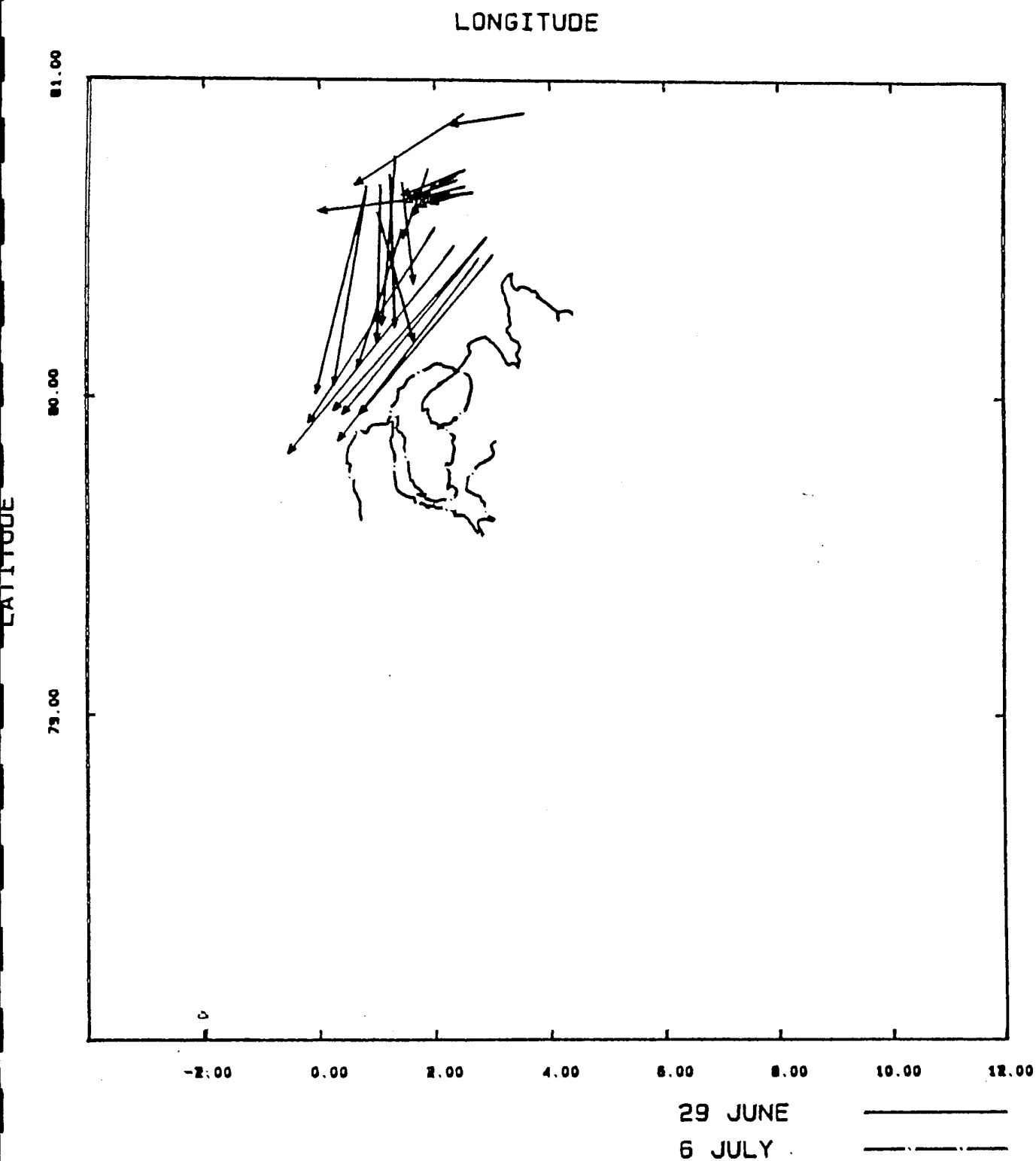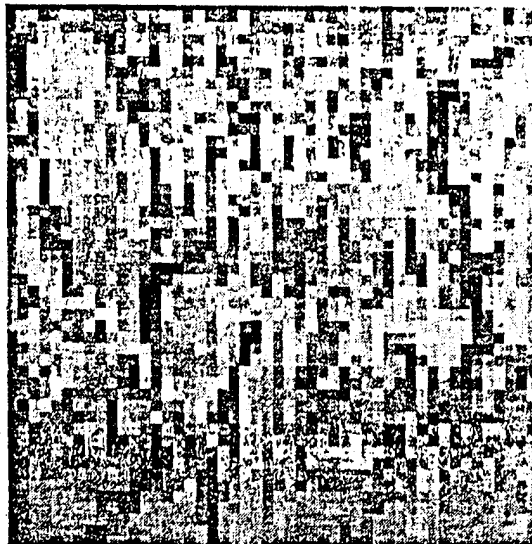# SAR EDGES/FLOE VECTORS: 29 - 6 JULY

Figure 9. SAR sea ice floe vector and edge generated from manual
interpretation of optically processed SAR data gathered
during MIZEX-84.

81 x 81 Pixel Average

27 x 27 Pixel Average

9 x 9 Pixel Average

Figure 10. Averaged images for Rev. 1482, for m=81, 27, and 9.
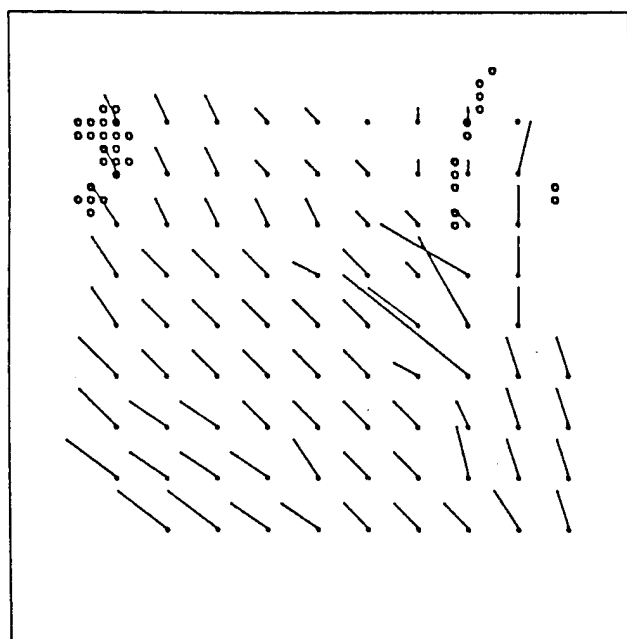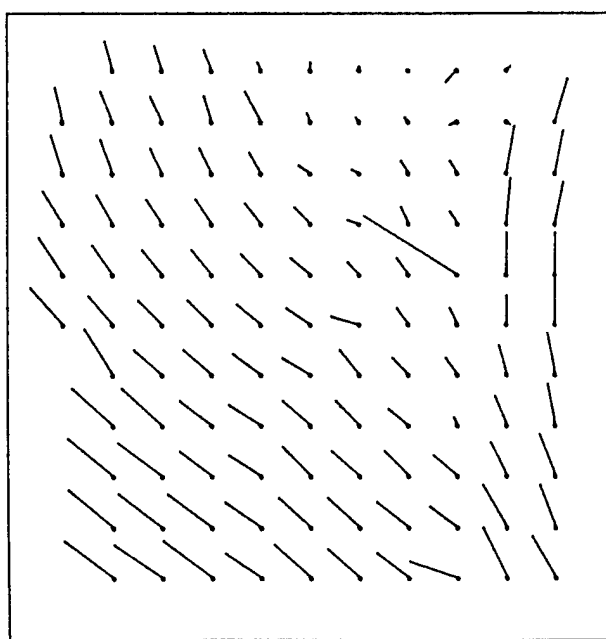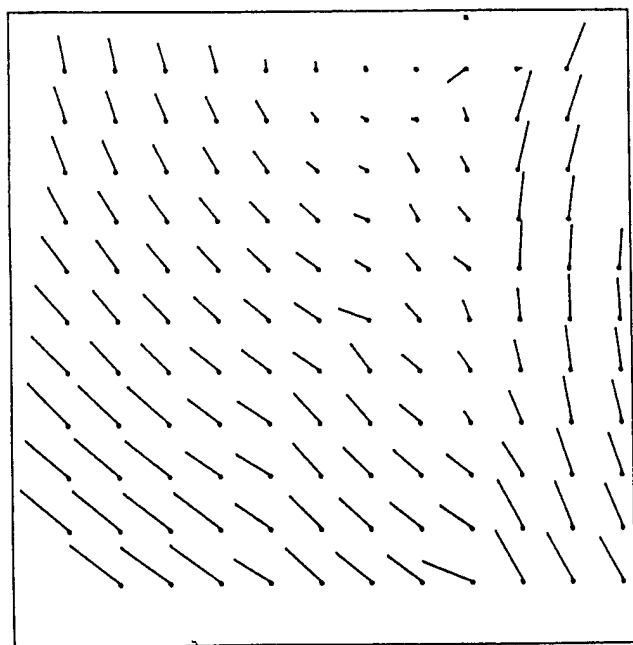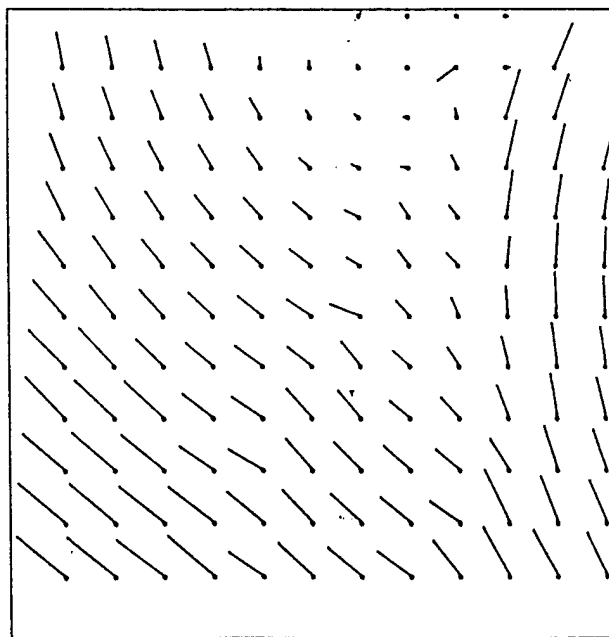
Figure 11. Displacement field (1 vector out of 4^2 shown) for different resolutions: $m = 81$, with seed tie points shown as circles, $m = 27$, $m = 9$, and $m = 3$. The displacements for $m = 1$ (not shown) are indistinguishable from those for $m = 3$. Actually, the scene from Rev. 1482 is 17.0 km downtrack from the scene from Rev. 1439 [5]; this uniform displacement must be added before any significance is attached to zeroes of the field.
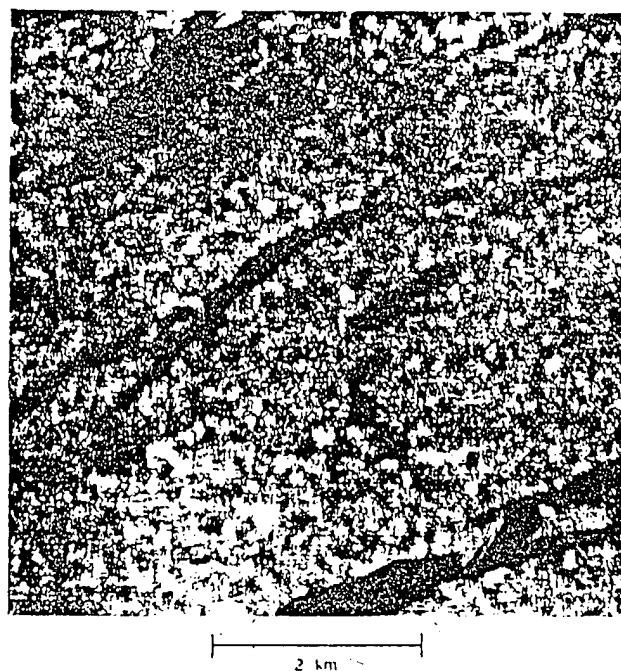
Figure 12a. STAR-1 image after smoothing by a median filter.

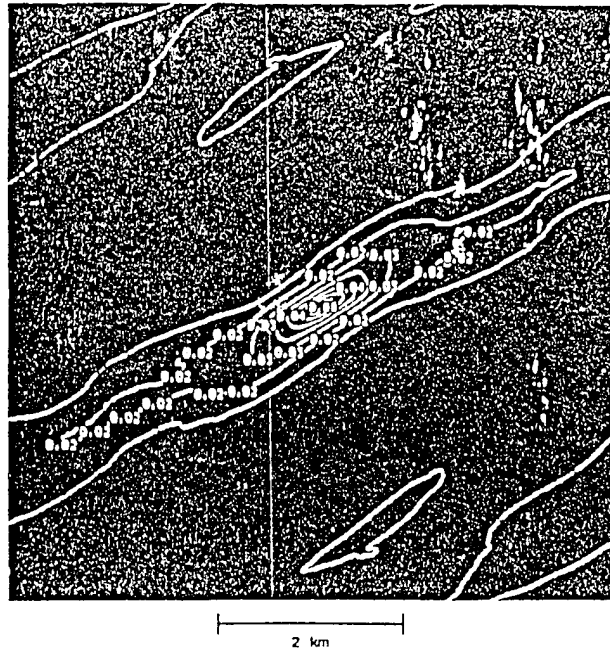Figure 12b. Binary image showing open-water leads.

Figure 12c. Contour plot of the autocorrelation function produced from the binary image shown in figure 12b.
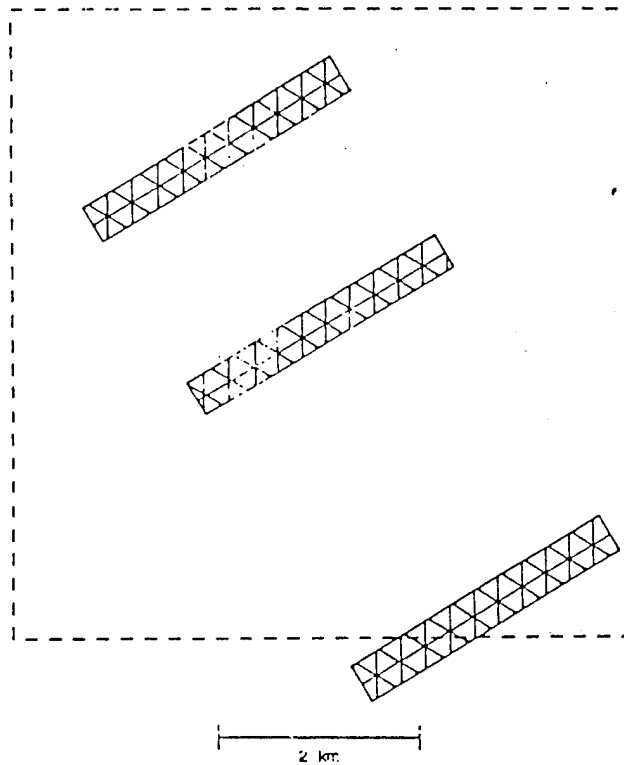

Figure 12d. One possible reconstruction of lead position from autocorrelation function.